AIAA 81-2458R

Liftoff Ignition Overpressure—A Correlation

E.J. Walsh* and P.M. Hart†
Martin Marietta Aerospace, Denver, Colorado

Current and planned launch vehicle configurations consist of extremely large vehicles requiring high-thrust propulsion systems for boost. A critical design condition for this type of vehicle is the pressure environment caused by the ignition start transient. The vehicle and surrounding support facilities must be designed to withstand these conditions. The resulting pressure wave emanating from the launch duct entrance can travel the entire length of the launch vehicle. This paper shows the results of full-scale measurements on several Titan vehicle launch conditions. Subscale model (Titan III) tests were also evaluated at a 7.5% model scale by NASA. The resultant correlation of subscale with full-scale data produces a scaling parameter that should be useful to vehicles such as shuttle and future launch vehicles with even larger thrust potentials.

Nomenclature

a_0 = ambient speed of sound
A = duct cross-sectional area
Kf = empirical constant pertaining to jet momentum
Km = empirical constant pertaining to jet mass
$\dot{m}$ = instantaneous mass flow rate
P_0 = ambient pressure
U_e = exhaust velocity
γ = ratio of specific heats
ρ_{e0} = density of exhaust gas at ambient pressure

Introduction

THE phenomenon of transient overpressures caused by engine ignition has long been recognized in missile and launch vehicle design. Pertinent analysis methods developed for the early Intercontinental Ballistic Missiles (ICBMs) (Atlas, Titan, and Minuteman)[1-4] were adapted for use with space launch vehicles such as the Titan III. Analysis methods developed for the silo-launched ICBMs proved adequate for defining a pressure pulse envelope for designing the base region of vehicles launched from surface launch mounts. These methods were not adequate for defining pulse attenuation above the launch mount. Therefore test data were required to evaluate the attenuation.

Special instrumentation was installed on the Titan launch pad (Fig. 1) for two launches. This instrumentation was installed at Launch Complex 41 for the TIIIE-05 flight and at Launch Complex 40 for the TIIIC-30 flight. Data obtained from these flights, together with limited data from Titan C-04, -07, -08, -11, -25, E-01, and E-02, provided the full-scale data base for the analysis covered in this report. The model data used in this report were obtained from a 7.5% scale model test[5] conducted by the National Aeronautics and Space Administration (NASA) at the Marshall Space Flight Center (MSFC).

A generalized mathematical model of the flow is derived from the methods originally provided by Broadwell and Tsu.[3]

The pressure waves propagating from the source region are given by

$$\Delta P = \frac{P_0}{2}\left[\left(\frac{\gamma \dot{m}}{a_0 \rho_{e0} A}\right) Km \pm \left(\frac{2u_e \dot{m}}{A}\right) Kf\right] \tag{1}$$

The plus sign is for the exhaust duct and the minus sign is for the launch duct. When the engine starts, exhaust gases flow into the source region at a rate assumed to be proportional to the engine chamber pressure. The flow is then considered a source of mass, momentum, and energy. The overpressure source is then calculated from the simultaneous solution of the conservation equations (mass, momentum, and energy), the gas equations of state, and the relationship between pressure and velocity across the pressure waves. Empirical factors obtained by experiments were used to describe the effects of the energy and momentum sources. Data from a 1/33 scale-model test[6] were used to substantiate the source region location for initial air displacement and to determine the values of the empirical volume ratio and momentum ratio factors. These factors, $Km = 2.0$ and $Kf = 0$, appear to be satisfactory for the initial compression wave pressure peaks. The source region of initial air displacement is located at the intersection of the nozzle centerline with the exhaust deflector.

The full-scale flight investigations were structured to enhance the information provided in the mathematical model previously described. Specifically, the flight vehicle instrumentation was designed to evaluate

1) the source pressures emanating from the launch duct;

2) the attenuation of the pressure wave as a function of distance from the source;

3) the waveform of the pressure pulse as a function of distance from the source;

4) the propagation speed of the pressure pulse;

5) the blockage effects induced by the launch mount structure; and

6) the degree of asymmetry in the pressures as they attenuate from the source.

The flight results obtained during the Titan III program were adequate to define all of these characteristics except the last item, the degree of asymmetry in the pressure pulse.

The subscale (7.5%) model tests were then planned to further quantify the flight results relative to these objectives. Another important objective of the subscale tests was to determine scale factors between subscale and full-scale tests for application to the STS program.

Presented as Paper 81-2458 at the AIAA/SETP/SFTE/SAE/ITEA/IEEE 1st Flight Testing Conference, Las Vegas, Nev., Nov. 11-13, 1981; submitted Nov. 24, 1981; revision received April 13, 1982.

*Technical Project Manager.
†Unit Head, Aerodynamics. Member AIAA.

Test Description

Flight Tests

Data from instrumentation on the launch pad and the umbilical mast (UM) are available from Titan flights C-04, -07, -08, -11, -25, -30, and E-05. Usable overpressure data were also obtained from airborne instrumentation on flights E-01 and E-02. Of these flights, the primary ignition launch overpressure effort was associated with vehicles C-30 and E-05. Since the instrumentation locations and designations were the same on both complexes, the following description is applicable to either complex. Twenty pressure measurements were installed on the transporter frame and the umbilical mast. Pressure measurements were concentrated primarily in the pitch plane of the vehicle and on the north UM. Pressure transducers were mounted either horizontally with the sensing port facing inward toward the solid rocket motor (SRM) or vertically with the sensing port facing downward. Instrumentation locations are shown in Figs. 2 and 3.

Airborne instrumentation installed for evaluation of compartment venting and skin pressure differentials on vehicles TIIIE-01 and E-02 was also used to evaluate the overpressure problem.

7.5% Model Scale

The model was configured to represent the four primary components of the Titan launch facility (LC-40) at Eastern Test Range (ETR)—the launch vehicle, exhaust duct, transporter frame, and umbilical mast. These were simulated in the tests.

The Launch Vehicle

A significant scaling parameter in establishing the model scale was the selection of Tomahawk motors to simulate the SRMs. Since the Tomahawk motor start transient provides a chamber pressure rise rate approximately 13 to 14 times that of the full-scale Titan SRM, a 7.5% model scale was selected. Launch vehicle lower stage components were then simulated on the linear scaling basis of 7.5% relative to the core and SRM motor diameters. Since the core engines are not ignited at liftoff, only the SRMs needed to be simulated for the Titan liftoff. The solid rocket motor parameters are compared in Table 1.

The launch vehicle core was simulated with a section of steel pipe. The base of the core vehicle (nozzles, boattail, etc.) was not simulated. The upper portion of the SRMs and the core vehicle could not be simulated because the SRM thrust was taken out through a thrust plate at the top of the fixture. This should not have affected the initial overpressure pulse but could have had an effect near the end of the overpressure pulse.

The Exhaust Duct

The exhaust duct entrance is a rectangular opening 18 × 58 ft in full scale. The deflector is a J-shaped section followed by a 27 × 42-ft horizontal duct. The model simulated the full-

Table 1 Solid rocket motor characteristics

	Full scale (Titan III SRM)	Model scale (Tomahawk)
Sea-level thrust, lb	1,170,000	10,600
Mass flow rate, lb/s	4700	45.88
Temperature (exit plane static), R	3300	...
Pressure (exit plane), psia	12.4	19
Nozzle cant angle, deg	6	...
Nozzle exit angle, deg	15	15
Nozzle exit Mach number	3.07	2.95
Nozzle exit area, ft^2	61.37	0.396
Nozzle area ratio	8:1	6.66:1

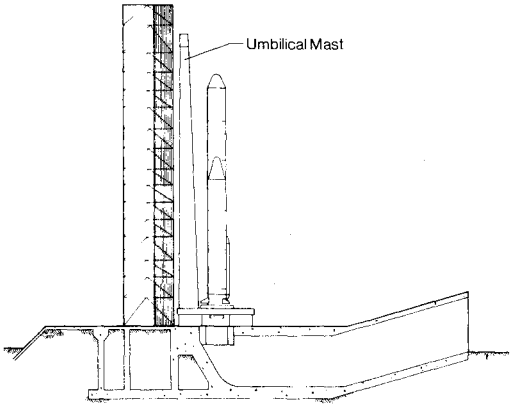

Fig. 1 Titan III launch stand schematic.

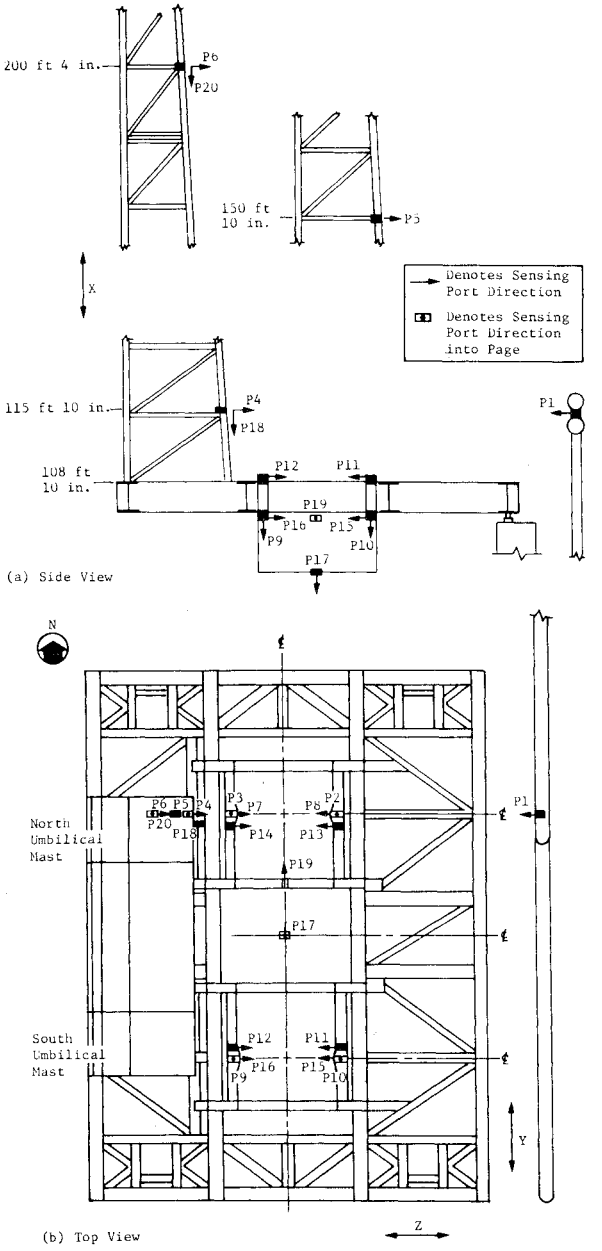

Fig. 2 Transporter frame and UM pressure instrumentation locations, flights C-30 and E-05.

scale configuration in all important aspects by using a steel duct covered with Fondu-Fyre (insulative coating).

The Transporter Frame

A transporter frame is centered over the exhaust duct. The upper side of the frame is 8 ft 10 in. above the pad surface level. The main members of the transporter are 3-ft-thick wide flange beams. The center portion of the frame under the liquid core of the launch vehicle is blocked by a pressure baffle (protecting the core engines from the overpressure pulse). The SRMs penetrate the plane of the transporter frame so the exhaust plane of the nozzle is 5 ft 8 in. below the top of the transporter frame. The model simulated the important features of the transporter dimensions as well as the location for instrumentation. Dimensional measurements were within 1% of the desired value.

The Umbilical Mast

The umbilical mast is a part of the transporter and rises approximately 154 ft above the pad. The mast is mounted in the transporter side opposite the exhaust duct location. The model dimensions were generally within 1% of the desired value.

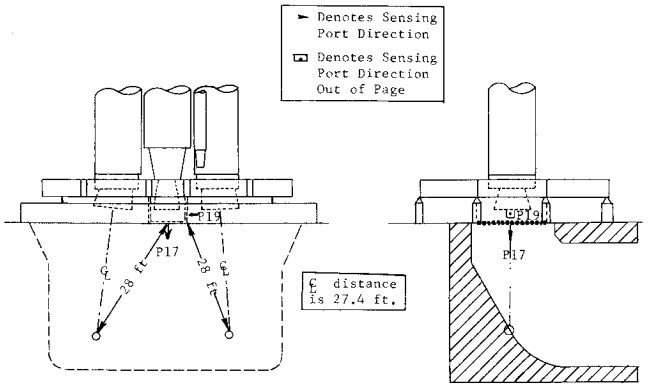

Fig. 3 Geometric relationship between instrumentation locations and SRM nozzles.

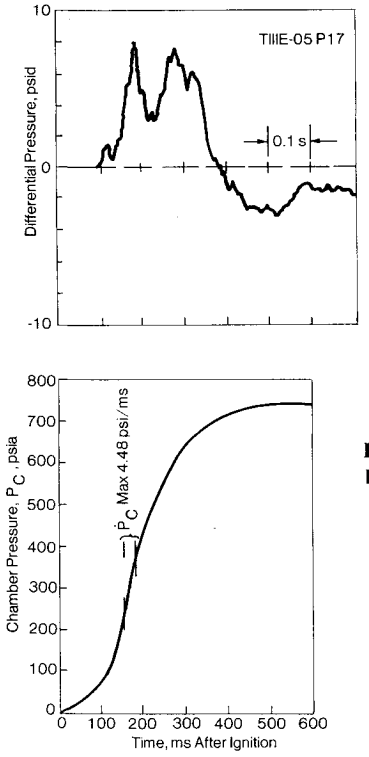

Fig. 4 Typical source pressure level and pulse characteristics.

Model Instrumentation

Overpressure instrumentation for the 7.5% scale model test consisted of 40 measurements. Launch stand instrumentation locations duplicated the full-scale C-30 and E-05 locations. Measurements on the simulated vehicle were located circumferential around the vehicle at stations which corresponded to the measurement location on the UM (station 115 ft 10 in., 150 ft 10 in., and 200 ft 4 in.).

Analysis and Discussion

The flight data are discussed in terms of the 20 measurements obtained during the E-05 and C-30 launch events. Supporting data from previous Titan-series flights are used to verify the characteristics of the overpressure phenomena indicated on these two flights.

Source Pressure Levels

Two pressure measurements, P-17 and P-19, were located near the predicted source of the pressure wave. These measurements were useful in establishing the pressure pulse characteristics and the source strength. Figure 4 illustrates the characteristic wave shape and the timing with respect to the SRM chamber pressure rise. Note that the compression wave is followed by an expansion wave due to rarefaction. The timing of the main compression pulse is consistent with the time of the peak SRM chamber pressure rise rate. Measurements P4, P5, P6, and P15 (Fig. 5) show the same characteristics and affirm the basic source strength.

Waveform

Typical launch overpressure pulse shapes are depicted in Fig. 6. The initial response of the transducer is noted approximately 100 ms after SRM ignition (depending on measurement location). The initial response is generally a small compression wave followed by a rarefaction wave. This is followed by the primary compression wave that peaks from about 70 to 80 ms after the initial response. Then, depending on the location and direction of the sensing port, the character

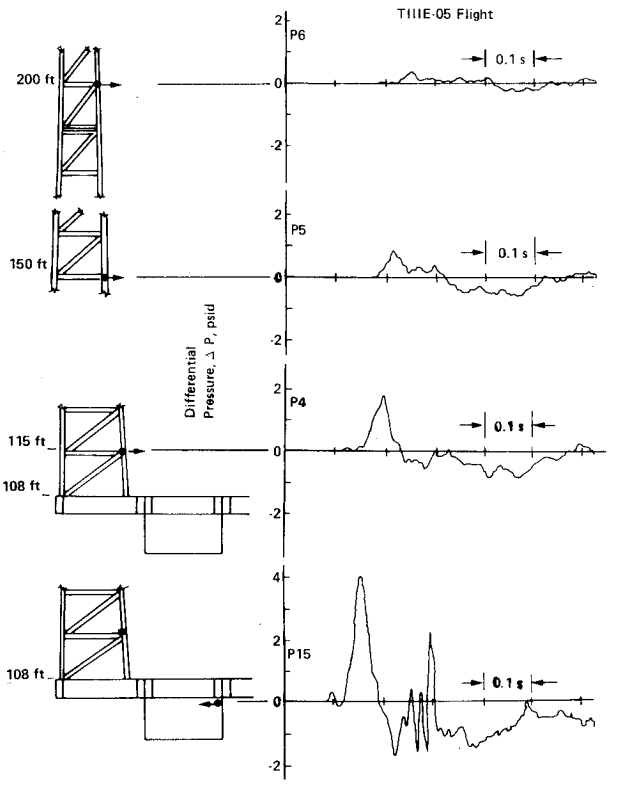

Fig. 5 Typical overpressure pulse characteristics.

of the pulse changes. For all instruments located above the transporter frame and for instruments below the transporter frame with a horizontal sensing direction, the pulse resembles that depicted in the upper portion of Fig. 6. The initial primary compression pulse is followed immediately by a rarefaction wave of approximately the same magnitude. For instruments located below the transporter frame with a vertical sensing direction, the initial compression is followed by multiple compression peaks caused by reflections within the duct and interactions between the vertical propagation of the pulse and the launch frame itself. This relatively high-amplitude long-duration (approximately 0.2 s) compression pulse is followed by a rarefaction wave with a magnitude generally less than one-half the compression wave. This type of pressure pulse appears to be characteristic of a loading on a surface normal to the direction of the overpressure wavefront. A typical wave shape for this type of pulse is presented in the lower portion of Fig. 6.

Wave Propagation

The strong correlation of the data gathered in these investigations shows that the pressure pulse travels at the local ambient speed of sound. Table 2 compares the propagation velocity between C-25, C-30, and E-05 launches. These data illustrate the timing of the initial pulse and the primary compression wave as previously discussed. The correlation between indicated propagation velocity and the local sonic velocity is excellent for C-30 and E-05, with a lesser degree of correlation for C-25.

Overpressure Pulse Attenuation

The effect of the SRM ignition overpressure pulse on the base of the vehicle is a primary design factor. The effects of the pulse on the remainder of the vehicle and on the launch complex must also be considered. Because of the transporter frame, missile, and UM, the wave does not propagate according to well-defined theories. Therefore attenuation is best defined by evaluating the test data within the bounds suggested by flow theory.

The attenuation of weak compression waves can be described by the relation

$$\Delta P = AX^{-B} \tag{2}$$

where B is dependent on the geometry involved, being 0, 0.5, and 1 for one-, two-, and three-dimensional waves, respectively; X is the distance from the source; and A is an empirical constant. The magnitude of the wave [(less than 5 differential pressure, pounds per square inch) (psid)] is not large enough to classify the generated disturbance as a blast wave or a strong compression wave with attendant larger exponents, e.g., 3 for a spherical blast wave. Since the duct opening is a rectangle (18×58 ft), the pressure wave might best be described by $B = 0.5$-1, with the actual value being a function of transporter design, wave blockage, and other effects. Analysis of the available data indicates that the appropriate source is the intersection of the SRM centerline (roll axis) extended to the plane of the duct opening (elevation 100 ft). The appropriate length for scaling attenuation appears to be radial distance (X_θ) from the source to the point in question.

The peak compression overpressure data (1-kHz filter) are presented in Fig. 7 as a function of X_θ. An appropriate scaling length for the pressures on the baffle could not be determined since the measurements lie between the two SRMs. Therefore these data as well as the measurements from the top of the transporter frame (partially shielded from the pressure wave) were ignored in deriving the attenuation equation. A curve of the form $\Delta P = AX^{-B}$ was fitted to the data. A least squares technique was used for the curve fit. As shown in the upper portion of Fig. 7, a reasonable representation of the data for the TIIIE-05 flight is obtained with $A = 23.3$, and $B = 0.754$. Note that the value of B falls between 0.5 and 1.0, as expected.

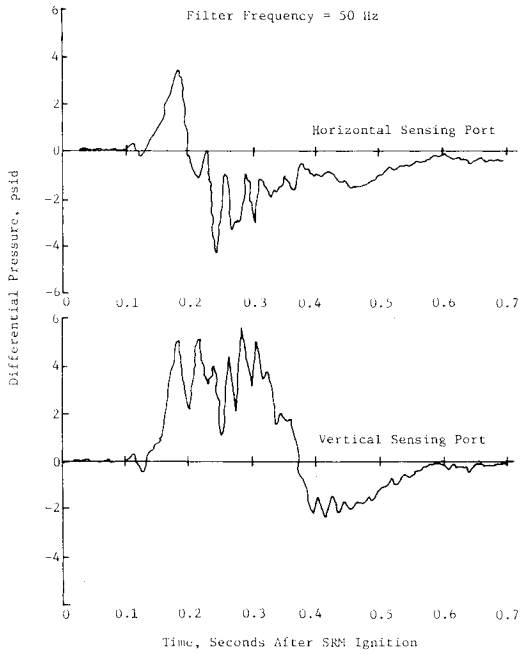

Fig. 6 Typical ignition overpressure pulse shapes.

Table 2 Overpressure pulse propagation velocity

Flight	Propagation velocity, ft/s	Local sonic velocity, ft/s
C-25	1087.0	1140.0
C-30	1123.9	1125.9
E-05	1111.1	1121.4

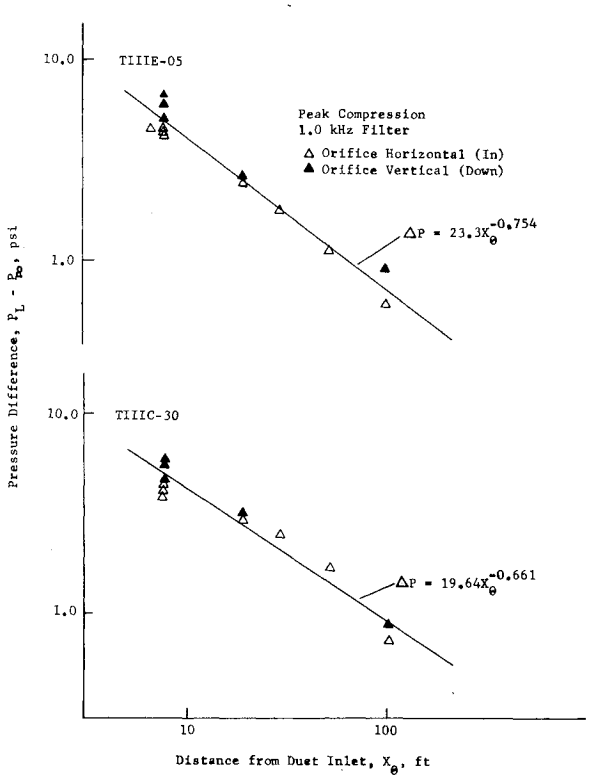

Fig. 7 Overpressure attenuation data, flights C-30 and E-05.

Data from the TIIIC-30 launch were analyzed using the same measurements as for TIIIE-05. These data are presented in the lower portion of Fig. 7. Coefficients for use in the attenuation relationship are $A=19.64$, $B=0.661$. These values compare reasonably well with those derived from the E-05 data. The C-30 and E-05 data were then combined to provide a larger data base to evaluate the attenuation. This combination of data produced the relationship

$$\Delta P=21.26X^{-0.706} \tag{3}$$

for the unmodified 1-kHz filtered data.

An effort was made to combine both the launch pad and airborne instrumentation data to evaluate the pressure wave attenuation. Use of a data base that included measurements from C-04, -07, -08, -11, -25, -30, E-01, E-02, and E-05 produced the relationship

$$\Delta P=30.52\,X^{-0.8707} \tag{4}$$

Figure 8 summarizes most of the flight data.

The overpressure values computed using the various relationships are compared in Table 3. These comparisons are for the "uncorrected" data. When dispersions such as varying SRM thrust rise rates, ambient temperatures, etc., are considered, it is felt that any of the relationships are adequate for engineering purposes.

The Titan III data obtained from both launch pad and airborne instrumentation indicate that the overpressure wave does attenuate according to the relationship $\Delta P=AX^{-B}$, where A and B are empirical constants determined from test data. The appropriate scaling parameter for X appears to be the radial distance from the centerline of the exhaust duct entrance to the point in question.

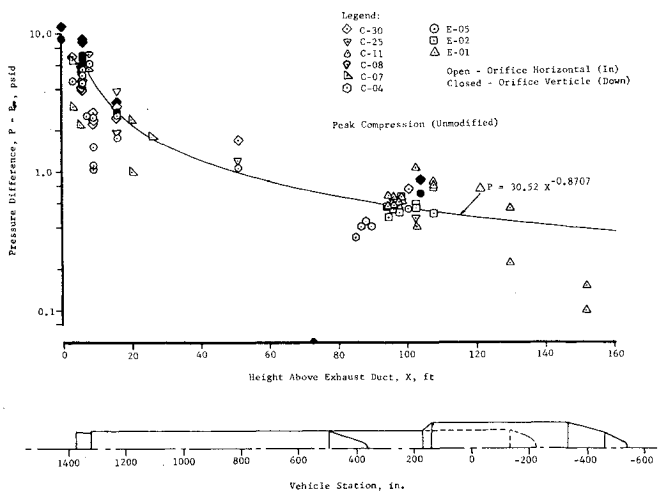

Fig. 8 Ignition overpressure attenuation data, TIIIC and TIIIE flights.

Asymmetry

Launch platform data indicate there is an asymmetry in the overpressure pulse below the transporter frame. The peak compression values for instruments located on the side opposite the UM, i.e., the east side, were higher than corresponding measurements on the UM side of the transporter. That is, it appears that asymmetry exists in the vehicle pitch plane. It was felt that if an asymmetry did exist, it should be evident in the filtered data since the high-frequency noise component would be eliminated. Comparison plots of the filtered data (Fig.9) confirm the presence of the asymmetry. Table 4, which presents peak overpressure values for the 1-kHz data, also confirms the asymmetry in the vehicle pitch plane. There is no discernible asymmetry in the yaw plane, however, because pressure transducers clustered around one SRM have peak values very similar to those of the comparable transducers around the other SRM.

The pitch plane asymmetry is thought to be the result of duct geometry. Sufficient flight data were not available to allow evaluation of asymmetries immediately above the transporter frame.

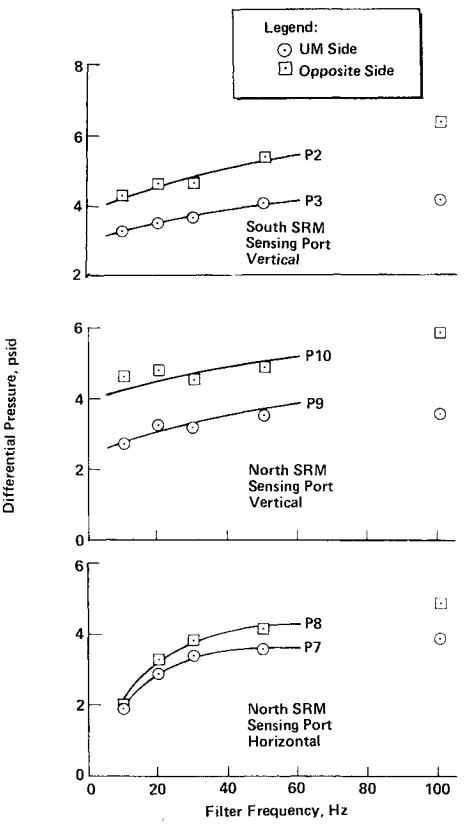

Fig. 9 Launch overpressure pulse asymmetry, transporter frame measurements.

Table 3 Calculated overpressure comparison

	E-05	C-30	E-05 + C-30	All available[a] (pad + airborne)
X, ft	$\Delta P=23.3\,X^{-0.754}$, psi	$\Delta P=19.6\,X^{-0.661}$, psi	$\Delta P=21.26\,X^{-0.706}$, psi	$\Delta P=30.52\,X^{-0.8707}$, psi
10	4.11	4.28	4.18	4.11
20	2.43	2.71	2.56	2.25
50	1.22	1.48	1.34	1.01
100	0.73	0.93	0.82	0.55

[a] Includes data from launches TIIIC-04, -07, -08, -11, -25, and -30 and TIIIE-01, -02, and -05.

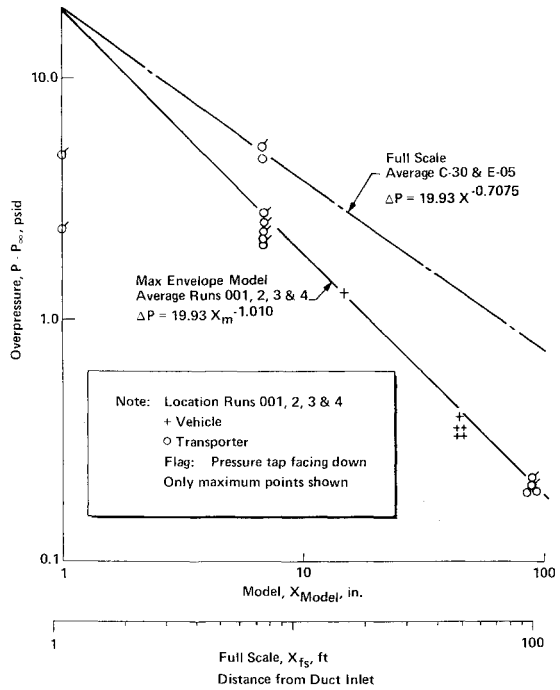

Fig. 10 Overpressure attenuation, model- and full-scale data.

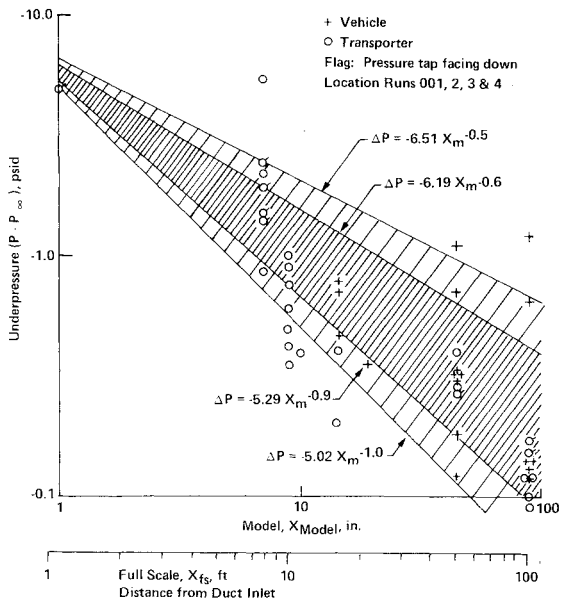

Fig. 11 Underpressure attenuation, 7.5% scale model data.

Table 4 Overpressure asymmetry comparison

Comparative measurements	Peak compression value,[a] psid		
	Sensing direction	UM side	Side opposite UM
P3, P2	Vertical	5.1	6.0
P7, P8	Horizontal	4.1	4.5
P9, P10	Vertical	4.9	6.6
P16, P15	Horizontal	4.2	4.8

[a] 1-kHz filtered data.

From the data available, a potential asymmetry exists in the vehicle pitch plane. An asymmetry of approximately 25% of the peak compression wave is possible near the base of the vehicle. The magnitude of the asymmetry near the top of the vehicle may be configuration-dependent.

Blockage

Peak compression data obtained from transducers mounted on top of the transporter frame were much less than those mounted beneath the frame because of the shielding provided by the transporter frame. Compression pressure peaks immediately above the transporter frame were approximately one-half those at similar locations below it.

Subscale Model Tests

The Titan III 7.5% scale-model test was structured to provide both acoustic and overpressure data at locations where full-scale data exist. Four separate tests were performed at the NASA MSFC facility in Huntsville, Alabama.[5] Test overpressure instrumentation included measurements at the locations shown in Figs. 2 and 3 as well as pressure measurements on the model launch vehicle.

The results of the subscale tests provide a qualitative comparison with the full-scale data. An in-depth analysis of the model data is not included here because of a lack of fidelity in some of the measurements. The criteria for selection of the data presented were predicated on the similarity of the pressure pulse waveform with that obtained from the flight results. The data presented are only for cases in which a relatively strong compression wave is followed by a rarefaction waveform.

Attenuation of the compression pulse was evaluated for each of the four model firings. Data from both transporter and vehicle measurements were bracketed (a constant source pressure was assumed). The exponent in the attenuation equation ($\Delta P = AX^{-B}$) varied from 0.996 to 1.056. The average attenuation from the model tests was

$$\Delta P = 19.93\, X^{-1.01} \tag{5}$$

Figure 10 summarizes the model compression pulse data. The full-scale attenuation curve developed from C-30 and E-05 data is presented for comparison. The model data were also used to evaluate attenuation of the rarefaction wave. These data are presented in Fig. 11. Using a best-fit curve for the individual firings resulted in exponents ranging from 0.808 to 0.689. The data were effectively enveloped with exponents ranging from 0.50 to 1.00. The bracketing equations shown in Fig. 11 result in a source rarefaction pressure approximately one-half the strength of the compression wave. This is consistent with the data observed from the full-scale firings.

Subscale/Full-Scale Correlations

The data comparison included here is limited because of the lack of fidelity in a portion of the model test data. It has been speculated that this lack of fidelity in the subscale data is due to 1) excessive time delays between the two solid motor starting conditions, and 2) instrumentation problems.

Attenuation

The subscale data generally provided an attenuation level higher ($B = 1.0$) than the flight results ($B = 0.75$). Qualitatively, however, it appears that both the flight and model data fall within the expected attenuation range ($B = 0.50$-1.0).

Amplitude

A quantitative comparison of the flight and subscale pressure levels is precluded by the lack of high-fidelity subscale model data. Figure 12 compares a portion of the model and flight compression pressure peaks. These data indicate that the subscale model data require amplification factors on the order of from 2 to 4 for agreement with full-scale pressures.

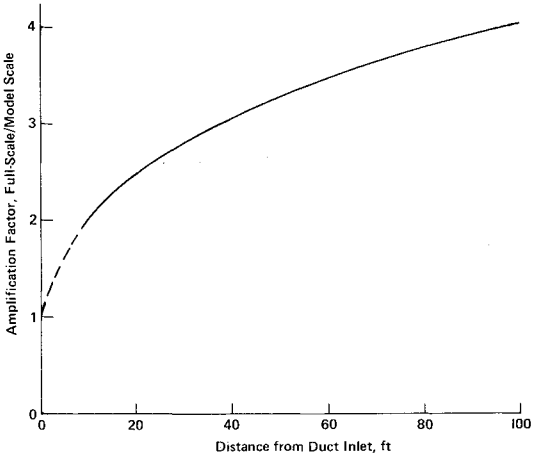

Fig. 12 Amplification factor for data correlation.

Waveform, Asymmetry, and Propagation

The full-scale data showed well-defined waveforms and a clearly delineated wave propagation level along with a limited amount of data to define asymmetry in the pressure pulse. Since the subscale data were not of sufficient fidelity to adequately define these parameters, no attempt was made to correlate these remaining parameters.

Conclusions

Evaluation of both the full-scale and the 7.5% model subscale data resulted in the following conclusions:

1) The amplitude of the ignition overpressures with regard to compression and rarefaction pressure levels is well-defined from the flight data. Qualitatively it would appear that amplification levels on the order of from 2 to 4 must be applied to the subscale data to maintain agreement with the flight data.

2) The attenuation of the pressure pulse can be defined by the relationship $\Delta P = AX^{-B}$, where B is within the range 0.5-1. Generally the subscale data were more strongly attenuated with distance from the source than were the flight data.

3) The waveforms observed on both the subscale and flight data were qualitatively comparable and exhibited the characteristic "N" waveforms.

4) Propagation of the pressure pulse is well defined from the full-scale data. The results provided show that the pressure wave travels at the local ambient speed of sound. The subscale data were not of sufficiently good fidelity to define the propagation levels.

5) Asymmetry of the ignition overpressures is partially defined in the full-scale data. The observed pressures on one side of the vehicle could be approximately 25% different from those on the opposite side of the vehicle. Data obtained from flight vehicle-mounted accelerometers and rate gyro data show significant perturbations, indicating an asymmetry in vehicle loading at the time of the ignition overpressure pulse. The subscale data were not adequate to further define the pressure asymmetries.

References

[1] Baltakis, P.F. and Opsahl, J.A., "Shock Tube Study of the Start-Up Pressure Pulse Phenomena in Four 1/30 Scale Atlas Flame Deflector Models," General Dynamics/Astronautics, San Diego, Calif., GDC-62-397, Dec. 1962.

[2] Buck, R.A., Combs, R.R., and Lays, E.J., "Launch Complex Acoustic and Aerothermodynamic Measurements, SSLV-05-7 Flight," Martin Marietta Corporation, Denver, Colo., SSLV-05-7 PER-1, Oct. 1965.

[3] Broadwell, J.E. and Tsu, C.N., "An Analysis of Transient Pressures Due to Starting in Underground Launchers," Space Technology Laboratories, El Segundo, Calif., 7103-0028-MU-000, June 1961.

[4] Bulk, G.K. and Parker, T.H., "Test Data Summary Report—Full-Scale (Minuteman) Launcher Tests for STM 101 through 111," TRW Space Technology Laboratories, El Segundo, Calif., STL/TR-60-0000-09218, Dec. 1960.

[5] Unpublished Data, NASA, Huntsvilla, Ala., 1977.

[6] Van Ert, D., McGregor, H.N., and Hart, P.M., "624A Scale Model Flame Deflector Program," Martin Marietta Corporation, Denver, Colo., Contract Item 13, Jan. 1963.